Three-dimensional edge plasma and neutral gas modeling with the EMC3-EIRENE code

on the example of RMP application in tokamaks - status and development plans

H. Frerichs, T. E. Evans, Y. Feng, D. Reiter and O. Schmitz

March 16-18, 2015 - Sherwood Fusion Theory Conference

THE UNIVERSITY of WISCONSIN MADISON

Motivation: Quantification of a 3D plasma edge

- One promising approach to **control particle and heat loads** onto divertor targets is the application of **resonant magnetic perturbations (RMPs)**.
- RMP application results in the formation of a **non-axisymmetric configuration**. $\rightarrow$ **3D modeling**
- Intrinsic error fields are non-axisymmetric as well!

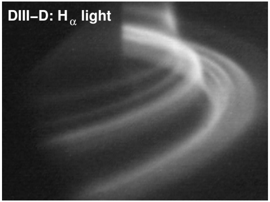

What we ultimately want to address:

- What is the impact of RMPs on detached divertor operation?

What do we need to do:

- Provide a reliable simulation model, at least of the same maturity as state of the art 2D models (e.g. SOLPS).

1. Introduction to EMC3-EIRENE

2. Overview on simulation results for DIII-D

3. Numerical access to high n_e, low T_e divertors

A 3D steady state fluid model for the edge plasma

Particle balance (n: plasma density)

$$\nabla \cdot \left[n u_{\|} \mathbf{e}_{\|} - D_{\perp} \mathbf{e}_{\perp} \mathbf{e}_{\perp} \cdot \nabla n \right] = S_p$$

$D_{\perp}$: anomalous cross-field diffusion, S_p: ionization of neutral particles

A 3D steady state fluid model for the edge plasma

Particle balance (n: plasma density)

$$\nabla \cdot \left[n u_{\parallel} \mathbf{e}_{\parallel} - D_{\perp} \mathbf{e}_{\perp} \mathbf{e}_{\perp} \cdot \nabla n \right] = S_p$$

$D_{\perp}$: anomalous cross-field diffusion, S_p: ionization of neutral particles

Momentum balance ($u_{\parallel}$: fluid velocity parallel to magnetic field lines)

$$\nabla \cdot \left[m_i n {u_{\parallel}}^2 \mathbf{e}_{\parallel} - \eta_{\parallel} \mathbf{e}_{\parallel} \mathbf{e}_{\parallel} \cdot \nabla u_{\parallel} - D_{\perp} \mathbf{e}_{\perp} \mathbf{e}_{\perp} \cdot \nabla \left(m_i n u_{\parallel} \right) \right] = -\mathbf{e}_{\parallel} \cdot \nabla n \left(T_e + T_i \right) + S_m$$

$\eta_{\parallel} \propto {T_i}^{5/2}$: parallel viscosity, $\eta_{\perp} = m_i n D_{\perp}$: cross-field viscosity,
S_m: interaction (CX) with neutral particles

A 3D steady state fluid model for the edge plasma

Particle balance (n: plasma density)

$$\nabla \cdot \left[n u_\parallel \mathbf{e}_\parallel - D_\perp \mathbf{e}_\perp \mathbf{e}_\perp \cdot \nabla n \right] = S_p$$

$D_\perp$: anomalous cross-field diffusion, S_p: ionization of neutral particles

Momentum balance ($u_\parallel$: fluid velocity parallel to magnetic field lines)

$$\nabla \cdot \left[m_i n {u_\parallel}^2 \mathbf{e}_\parallel - \eta_\parallel \mathbf{e}_\parallel \mathbf{e}_\parallel \cdot \nabla u_\parallel - D_\perp \mathbf{e}_\perp \mathbf{e}_\perp \cdot \nabla \left(m_i n u_\parallel \right) \right] = -\mathbf{e}_\parallel \cdot \nabla n \left(T_e + T_i \right) + S_m$$

$\eta_\parallel \propto {T_i}^{5/2}$: parallel viscosity, $\eta_\perp = m_i n D_\perp$: cross-field viscosity,
S_m: interaction (CX) with neutral particles

Energy balance (T_e, T_i: electron and ion temperature)

$$\begin{aligned}
\nabla \cdot \left[\frac{5}{2} T_e \left(n u_\parallel \mathbf{e}_\parallel - D_\perp \mathbf{e}_\perp \mathbf{e}_\perp \cdot \nabla n \right) - \left(\kappa_e \mathbf{e}_\parallel \mathbf{e}_\parallel + \chi_e n \mathbf{e}_\perp \mathbf{e}_\perp \right) \cdot \nabla T_e \right] &= +k \left(T_i - T_e \right) + S_{ee} \\
\nabla \cdot \left[\frac{5}{2} T_i \left(n u_\parallel \mathbf{e}_\parallel - D_\perp \mathbf{e}_\perp \mathbf{e}_\perp \cdot \nabla n \right) - \left(\kappa_i \mathbf{e}_\parallel \mathbf{e}_\parallel + \chi_i n \mathbf{e}_\perp \mathbf{e}_\perp \right) \cdot \nabla T_i \right] &= -k \left(T_i - T_e \right) + S_{ei}
\end{aligned}$$

$\kappa_{e,i} \propto {T_{e,i}}^{5/2}$: classical parallel heat conductivity, χ_e, χ_i: anomalous cross-field transport,
$k \propto n^2 \, {T_e}^{-3/2}$: energy exchange between el. and ions,
S_{ee}, S_{ei}: interaction with neutral particles and impurities (radiation)

A Monte Carlo method for fluid edge plasmas

- Balance equations can be cast in generic Fokker-Planck form:

$$\frac{\partial}{\partial t}\mathcal{F} + \nabla\cdot\left[\boldsymbol{\mathcal{V}}\,\mathcal{F} - \nabla\cdot\boldsymbol{\mathcal{D}}\mathcal{F}\right] = \mathcal{S} \tag{1}$$

  with corresponding drift ($\boldsymbol{\mathcal{V}}$) and diffusion ($\boldsymbol{\mathcal{D}}$) coefficients and sources/sinks ($\mathcal{S}$).
- (1) is related to a **stochastic process** $\rightarrow$ apply Monte Carlo method: follow "fluid particles" from source to sink.
- The motion of simulation particles is determined by the coefficients $\boldsymbol{\mathcal{V}}$ and $\boldsymbol{\mathcal{D}}$ and numerical time step τ. Along field lines we have:

$$\Delta\, l_{\parallel} = \boldsymbol{\mathcal{V}}_{\parallel}\,\tau + \sqrt{2\,\boldsymbol{\mathcal{D}}_{\parallel}\,\tau}\,\xi, \qquad \langle\xi\rangle = 0, \quad \left\langle\xi^2\right\rangle = 1 \tag{2}$$

A Monte Carlo method for fluid edge plasmas

- Balance equations can be cast in generic Fokker-Planck form:

$$\frac{\partial}{\partial t}\mathcal{F} + \nabla \cdot \left[\boldsymbol{\mathcal{V}}\,\mathcal{F} - \nabla \cdot \boldsymbol{\mathcal{D}}\mathcal{F}\right] = \mathcal{S} \qquad (1)$$

  with corresponding drift ($\boldsymbol{\mathcal{V}}$) and diffusion ($\boldsymbol{\mathcal{D}}$) coefficients and sources/sinks ($\mathcal{S}$).
- (1) is related to a **stochastic process** $\rightarrow$ apply Monte Carlo method: follow "fluid particles" from source to sink.
- The motion of simulation particles is determined by the coefficients $\boldsymbol{\mathcal{V}}$ and $\boldsymbol{\mathcal{D}}$ and numerical time step τ. Along field lines we have:

$$\Delta\, l_{\parallel} = \boldsymbol{\mathcal{V}}_{\parallel}\,\tau + \sqrt{2\,\boldsymbol{\mathcal{D}}_{\parallel}\,\tau}\,\xi, \qquad \langle \xi \rangle = 0, \quad \left\langle \xi^2 \right\rangle = 1 \qquad (2)$$

- Classical parallel heat conduction ($q_{\parallel} = -\kappa_{\parallel}\,\nabla_{\parallel}\,T, \qquad \kappa_{\parallel} \sim T^{5/2}$):

$$q_{\parallel} = -\nabla_{\parallel}\,\underbrace{\kappa_{\parallel}}_{\boldsymbol{\mathcal{D}}}\,T + T\,\underbrace{\nabla_{\parallel}\,\kappa_{\parallel}}_{\boldsymbol{\mathcal{V}}} = -\nabla_{\parallel}\,\underbrace{\frac{2\,\kappa_{\parallel}}{7}}_{\boldsymbol{\mathcal{D}}'}\,T \qquad (3)$$

Self-consistent solution by iterative application

- Input for EMC3-EIRENE:
  - User-defined boundary conditions: n_{ISB} or Γ_{rec} or $(\Gamma_{\text{in}}, \varepsilon_{\text{pump}})$, P_{in}.
  - User-defined model parameters: $D_\perp$, $\chi_{e\perp}$, $\chi_{i\perp}$.
- Built-in boundary conditions: c_s at target, sheath heat transmission coefficients γ_e, γ_i.
- A relaxation factor α_{rlx} needs to be introduced because of the strong non-linearity:

$$\mathcal{F}_{n,\text{rlx}} = \alpha_{\text{rlx}} \, \mathcal{F}_{n-1} + (1 - \alpha_{\text{rlx}}) \, \mathcal{F}_n$$

- Approximate convergence: small changes between iterations at intrinsic noise level.

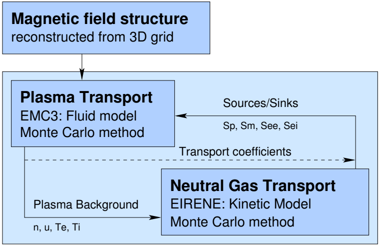

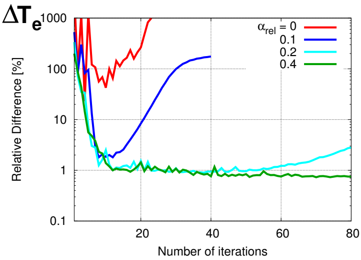

The field line reconstruction module allows geometric flexibility

- Magnetic field lines are reconstructed from a 3D finite flux-tube grid (bilinear interpolation).

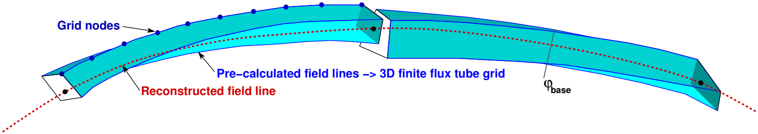

- The 3D grid is generated by field lines tracing starting from 2D base grids.

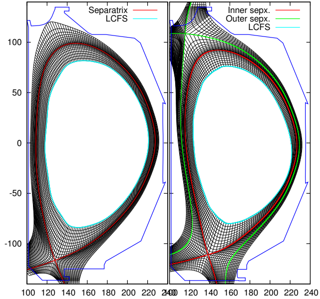

$\rightarrow$ finite flux-tube length for good cross-section.

- Discretization in the cross-field direction can be adapted to the magnetic configuration at hand.
- Single null and disconnected double null configurations available.
  Application: DIII-D, MAST, JET, ITER, . . .
- Easy to setup advanced magnetic divertor configurations (Super-X or Snowflake).

An ITER similar shape plasma at DIII-D

Vacuum RMP configuration:

- Magnetic field structure at the plasma edge: island chains, chaotic regions, short flux tubes.
- The perturbed separatrix introduces a helical deformation of the regular SOL, and guides field lines to a non-axisymmetric divertor footprint.

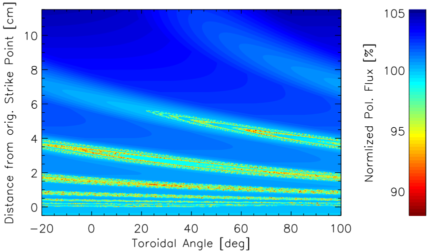

DIII-D discharge 132741: $I_c = 4\,\mathrm{kA}(n = 3)$

$B_t = 1.8\,\mathrm{T}$, $I_p = 1.5\,\mathrm{MA}$, $q_{95} = 3.5$

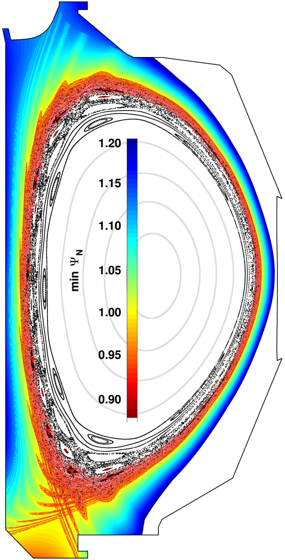

Discrepancy between simulations and experiments

DIII-D: ITER similar shape H-mode plasma at low collisionality

- **Experiment:** Striation pattern in particle loads, but **not** in heat loads. Moderate temperature reduction by RMPs.
- **Simulation:** Striation pattern in both particle and heat loads. Significant temperature reduction by RMPs.

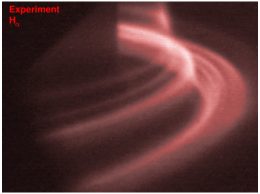

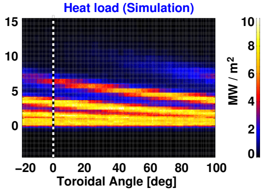

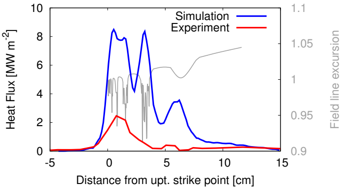

- Possible reasons for this discrepancy:
  1. “Kinetic corrections” to fluid model necessary at low collisionalities?
  2. Partial screening of RMPs by plasma response?
  3. Recycling conditions?

1. Adjust el. heat conduction at low collisionalities

- An upper limit is given by free streaming particles (with thermal velocity):

$$q_{\mathrm{lim}} = \alpha_e \, n_e \, v_{th,e} \, T_e, \qquad \alpha_e \approx 0.03 \ldots 0.15.$$

- This can be related to a correction factor β for the heat conductivity:

$$\kappa^*_{\parallel e} = \beta \, \kappa_{\parallel e}, \qquad \beta = \left(1 + \frac{\kappa_{\parallel e} \, |\nabla_\parallel T_e|}{q_{\mathrm{lim}}}\right)^{-1} \leq 1.$$

- Explore the impact of a reduced $\kappa_{\parallel e}$, **set fixed value for** β:

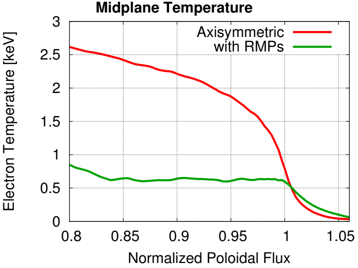

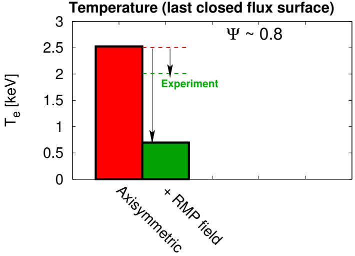

1. Adjust el. heat conduction at low collisionalities

- An upper limit is given by free streaming particles (with thermal velocity):

$$q_{\lim} = \alpha_e \, n_e \, v_{th,e} \, T_e, \qquad \alpha_e \approx 0.03 \ldots 0.15.$$

- This can be related to a correction factor β for the heat conductivity:

$$\kappa^*_{\parallel e} = \beta \, \kappa_{\parallel e}, \qquad \beta = \left(1 + \frac{\kappa_{\parallel e} \, |\nabla_\parallel T_e|}{q_{\lim}}\right)^{-1} \leq 1.$$

- Explore the impact of a reduced $\kappa_{\parallel e}$, **set fixed value for** β:

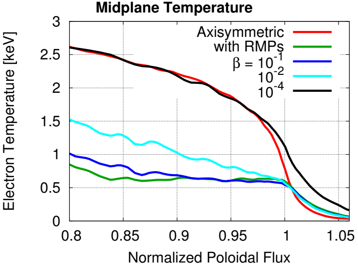

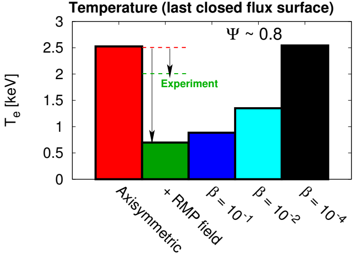

- A correction of $\beta \sim 10^{-3}$ is required to be consistent with an experimentally observed temperature reduction of $\sim 20\,\%$.

2. Approximation of screening of RMPs

- The plasma may screen external magnetic perturbations, which would result in a modification of the magnetic field structure.
- A helical current sheet model has been used to explore the impact of RMP screening by plasma response. Here: $m = 7 - 11$ resonances are screened:

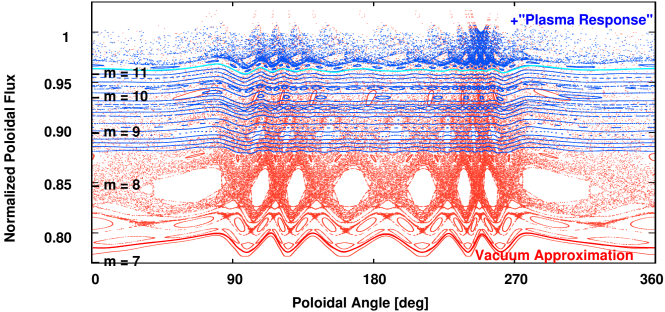

- $\Rightarrow$ The open chaotic layer is limited to the very edge (~ 0.96).

Screening of RMPs cannot be too strong!

H. Frerichs et al., Phys. Plasmas **19**, 052507 (2012)

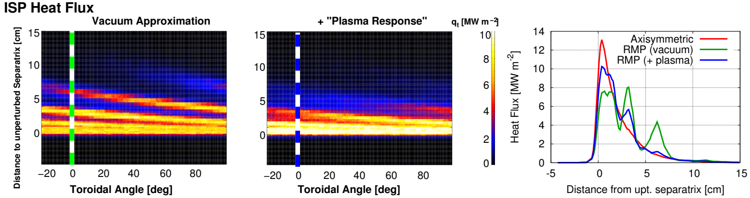

- The striation patterns of particle and heat loads follow the magnetic field structure. → Secondary peaks are reduced with “plasma response”.
- While this gives better agreement for the heat loads, it is against experimental observations regarding the particle load!

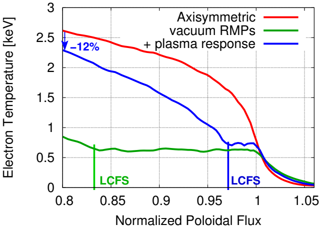

- The plasma response is consistent with a core temperature drop of 20 % in the experiment.
- A plateau remains in the (reduced) open field line region.
  → combination of moderate screening and heat flux limit?

3. Recyling conditions can explain the qualitative difference between particle and heat flux pattern

- The pumping parameter ε_{pump} allows to control recycling conditions (although it is determined by the present pump setup).
- Reducing ε_{pump} to small values significantly increases the total recycling flux, but the splitting into primary and secondary peaks remains.

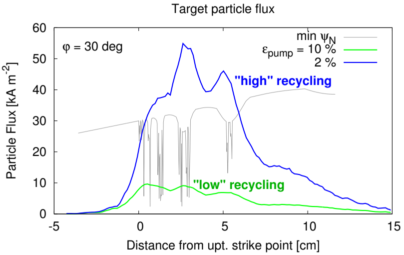

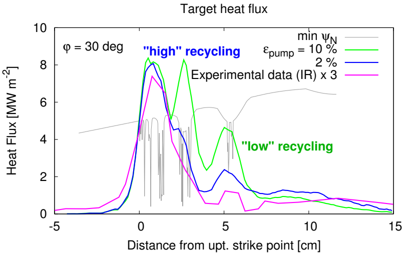

H. Frerichs et al., Phys. Plasmas **21**, 020702 (2014)

- The secondary heat flux peaks “detach” under (artificial?) high-recycling conditions. But peak level is still too high (“radiation shortfall”)!

Numerical access to detachment: generalize coupling between EMC3 and EIRENE

- Include neutral **gas-puffing** and **volume recombination**.
  $\rightarrow$ Particle balance from plasma (EMC3) and neutral gas (EIRENE) point of view:

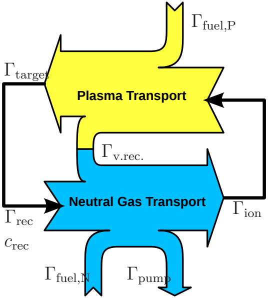

$$\Gamma_{\mathrm{fuel,P}} + \Gamma_{\mathrm{ion}} = \Gamma_{\mathrm{target}} + \Gamma_{\mathrm{vol.\ rec.}}$$
$$\Gamma_{\mathrm{rec}} + \Gamma_{\mathrm{fuel,N}} + \Gamma_{\mathrm{vol.\ rec.}} = \Gamma_{\mathrm{pump}} + \Gamma_{\mathrm{ion}}$$

- Different operation modes available: set control parameter Γ_{tot}, n_{ISB} or c_{rec} allows explicit (Γ_{pump}) and implicit ($c_{\mathrm{rec}} < 1$) treatment of particle sinks.

- Stable access to high density, low temperature divertor conditions remains an issue: oscillations occur even before volume recombination is switched on.

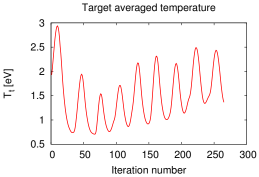

Numerical instability related to simulation procedure?

- The transport solver (EMC3-EIRENE) is a **non-linear operator**

$$\Phi_{\text{EMC3-EIRENE}} : \mathcal{P} \to \mathcal{P}', \qquad \mathcal{P} = \left\{ n(\mathbf{x}), M(\mathbf{x}), T_e(\mathbf{x}), T_i(\mathbf{x}) \right\}$$

  which maps the plasma state $\mathcal{P}$ to $\mathcal{P}'$ (because transport coefficients and sources depend on $\mathcal{P}$).
- For a self consistent plasma solution we need to find a **fixed-point**

$$\mathcal{P}^* = \Phi_{\text{EMC3-EIRENE}}(\mathcal{P}^*)$$

- The simulation procedure resembles an iterative approximation

$$\mathcal{P}_{n+1} = \Phi_{\text{EMC3-EIRENE}}(\mathcal{P}_n) \qquad \text{until} \quad \|\mathcal{P}_{n+1} - \mathcal{P}_n\| \leq C$$

- However, "complicated" dynamics is a well known feature of non-linear maps.

Two-point model analysis of the simulation procedure

- Oscillations of the plasma state occur when the divertor temperature **drops below a few** eV.
- This behavior can be captured within a two-point model (2PM) analysis of the simulation procedure ($\mathcal{P}_{n+1} = \Phi_{\text{EMC3-EIRENE}}(\mathcal{P}_n)$):

$$
\begin{aligned}
2\, n_t\, T_t &= f_{\text{mom}}\, n_u\, T_u && (4)\\
T_u^{7/2} &= T_t^{7/2} + \frac{7\, f_{\text{cond}}\, q_{||}\, L}{2\, \kappa_{0e}} && (5)\\
(1 - f_{\text{power}})\; q_{||} &= \gamma\, e\, n_t\, T_t\, c_{st} && (6)
\end{aligned}
$$

u: upstream $\sim$ midplane

- Account for T_t and n_t dependence in f_{power}, f_{mom} and f_{cond}
- A relaxation factor α is applied in the simulations with the intention to stabilize the iterative procedure:

$$Q'_{n+1} \mapsto \alpha Q_n + (1-\alpha)\, Q_{n+1})$$

Two-point model analysis of the simulation procedure

- Oscillations of the plasma state occur when the divertor temperature **drops below a few** eV.
- This behavior can be captured within a two-point model (2PM) analysis of the simulation procedure ($\mathcal{P}_{n+1} = \Phi_{\text{EMC3-EIRENE}}(\mathcal{P}_n)$):

$$
\begin{aligned}
T_{t,(n+1)} &= \frac{(1 - f_{\text{power}})\; q_{||}}{\gamma\; e\; n_t\; c_{st}(T_{t,(n)})} \\
T_{u,(n+1)} &= \frac{1}{T_{u,(n)}^{5/2}} \left[T_{t,(n)}^{5/2}\; T_{t,(n+1)} + \frac{7\, f_{\text{cond}}\; q_{||}\; L}{2\; \kappa_{0e}} \right] \\
n_{t,(n+1)} &= \frac{f_{\text{mom}}\; n_u\; T_u}{2\; T_t}.
\end{aligned}
$$

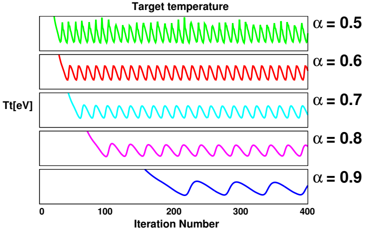

- Account for T_t and n_t dependence in f_{power}, f_{mom} and f_{cond}
- A relaxation factor α is applied in the simulations with the intention to stabilize the iterative procedure:

$$
Q'_{n+1} \mapsto \alpha Q_n + (1 - \alpha)\, Q_{n+1})
$$

Two-point model analysis of the simulation procedure

- Oscillations of the plasma state occur when the divertor temperature **drops below a few** eV.
- This behavior can be captured within a two-point model (2PM) analysis of the simulation procedure ($\mathcal{P}_{n+1} = \Phi_{\text{EMC3-EIRENE}}(\mathcal{P}_n)$):

$$
\begin{aligned}
T_{t,(n+1)} &= \frac{(1 - f_{\text{power}})\ q_{||}}{\gamma\ e\ n_t\ c_{st}(T_{t,(n)})} \\
T_{u,(n+1)} &= \frac{1}{T_{u,(n)}^{5/2}} \left[T_{t,(n)}^{5/2}\ T_{t,(n+1)} + \frac{7\ f_{\text{cond}}\ q_{||}\ L}{2\ \kappa_{0e}} \right] \\
n_{t,(n+1)} &= \frac{f_{\text{mom}}\ n_u\ T_u}{2\ T_t}.
\end{aligned}
$$

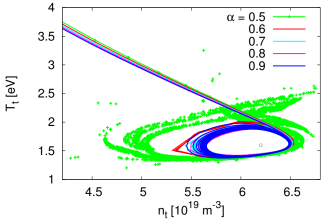

- Account for T_t and n_t dependence in f_{power}, f_{mom} and f_{cond}
- A relaxation factor α is applied in the simulations with the intention to stabilize the iterative procedure:

$$Q'_{n+1} \mapsto \alpha Q_n + (1 - \alpha)\, Q_{n+1})$$

Convergence control by adaptive relaxation

- The orbits in n_t-T_t space are rather robust with respect to the relaxation factor, however, the frequency of the cycle $\Omega \to 0$ for $\alpha \to 1$.

- An **adaptive relaxation** method is motivated by the character of the cycle in n_t-T_t space:
  1. weak relaxation for T_t in quad. 1 and 3
  2. strong relaxation for T_t in quad. 2 and 4

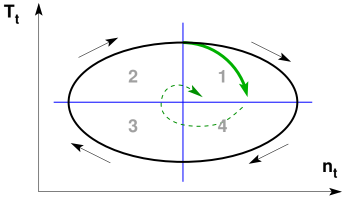

- Analyze history of n_t and T_t to approximate the phase φ_n. Then apply adaptive relaxation:

$$\alpha_n = \alpha_{\text{weak}} + \left(\alpha_{\text{strong}} - \alpha_{\text{weak}}\right) A_n, \qquad A_n = \frac{1}{2}\left(1 \pm \sin(2\,\varphi_n)\right)$$

Convergence control by adaptive relaxation

- The orbits in n_t-T_t space are rather robust with respect to the relaxation factor, however, the frequency of the cycle $\Omega \to 0$ for $\alpha \to 1$.

- An **adaptive relaxation** method is motivated by the character of the cycle in n_t-T_t space:
  1. weak relaxation for T_t in quad. 1 and 3
  2. strong relaxation for T_t in quad. 2 and 4

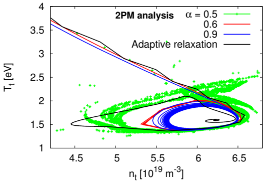

- Analyze history of n_t and T_t to approximate the phase φ_n. Then apply adaptive relaxation:

$$\alpha_n = \alpha_{\text{weak}} + \left(\alpha_{\text{strong}} - \alpha_{\text{weak}}\right) A_n, \qquad A_n = \frac{1}{2}\left(1 \pm \sin(2\,\varphi_n)\right)$$

Convergence control by adaptive relaxation

- The orbits in n_t-T_t space are rather robust with respect to the relaxation factor, however, the frequency of the cycle $\Omega \to 0$ for $\alpha \to 1$.

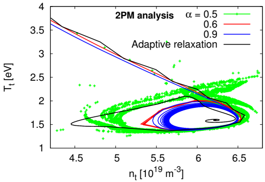

- An **adaptive relaxation** method is motivated by the character of the cycle in n_t-T_t space:
  1. weak relaxation for T_t in quad. 1 and 3
  2. strong relaxation for T_t in quad. 2 and 4

- Analyze history of n_t and T_t to approximate the phase φ_n. Then apply adaptive relaxation:

$$\alpha_n = \alpha_{\text{weak}} + \left(\alpha_{\text{strong}} - \alpha_{\text{weak}}\right) A_n, \qquad A_n = \frac{1}{2}\left(1 \pm \sin(2\,\varphi_n)\right)$$

- Such an adaptive relaxation scheme is straightforward to implement into the EMC3-EIRENE code as a **post-processing** subroutine, although **robustness** is still an issue for complex 3D simulations.

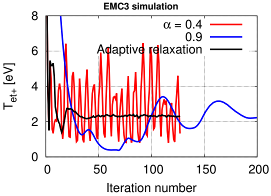

H. Frerichs et al., Comput. Phys. Commun. **188**, 82 (2015)

Summary and conclusions

- The experimentally observed pattern of divertor particle and heat fluxes can be reconstructed by adjusting the recycling conditions.
- Some discrepancies remain regarding the global power balance and pumping efficiency (boundary condition).
- Model extensions require (at least) a formulation of a “heat flux limit” suitable for Monte Carlo methods, and coupling to realistic modeling of MHD effects (plasma response from M3D-C1, NIMROD, VMEC).
- An adaptive relaxation method has been proposed to stabilize simulations at high divertor density and very low temperatures, with promising results for application in EMC3-EIRENE.

Extended operation mode of EMC3-EIRENE

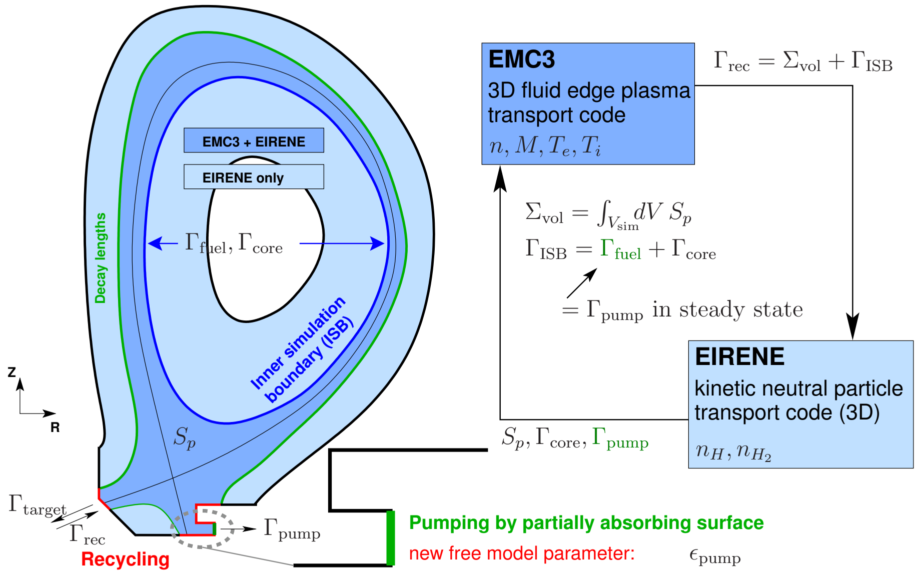

The overestimation of the peak heat flux is related to missing/underestimated other power losses

- The experimental **steady state** power balance at DIII-D (ISS H-mode plasmas, ELM suppression by RMPs): $P_{\text{in}} = 6 - 8\,\mathrm{MW}$ edge input power
- Very weak striation pattern from RMPs: (shot 132741: Schmitz, JNM **415** (2011) S886)

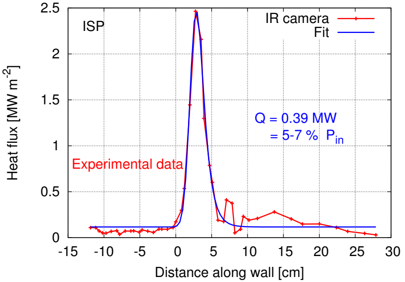

- Power deposition profile can be fitted to generic formula:

  (Eich, PRL **107**, 215001 (2011))

$$q(\bar{s}) = \frac{q_0}{2}\ \exp\left[\left(\frac{S}{2\,\lambda_q\,f_x}\right)^2 - \frac{\bar{s}}{\lambda_q\,f_x}\right]\ \text{erfc}\left[\frac{S}{2\,\lambda_q\,f_x} - \frac{\bar{s}}{S}\right] + q_{BG}$$

- Integral: $Q \approx 2\pi R_0\,\lambda_q\,f_x\,q_0$

- **Some power losses unaccounted for? (Radiation, fast particles?)**
- “Radiation shortfall” is a known issue in 2D simulations.

Implementation of heat flux limit in Monte Carlo scheme

- Adapted parallel heat flux: $q_{\parallel} = -\beta\,\kappa_{\parallel}\,\nabla_{\parallel}\,T_e$

$$q_{\parallel} = -\nabla_{\parallel} \underbrace{\frac{2\,\beta\,\kappa_{\parallel}}{7}}_{\mathcal{D}} T_e + T_e \underbrace{\frac{-2\,\beta\,\kappa_{\parallel}}{7} \nabla_{\parallel} \ln\beta}_{\mathcal{V}} \tag{4}$$

- Direct implementation (explicit):

$$\Delta\, l_{\parallel} = \mathcal{V}_{\parallel}\,\tau + \underbrace{\sqrt{2\,\mathcal{D}_{\parallel}\,\tau}\,\xi}_{l_1} \tag{5}$$

- Two-step method (implicit, predictor-corrector): $\Delta\, l_{\parallel} = l_1 + l_2$

$$l_2 = l_1 \left(\sqrt{1-\Delta} - 1\right), \qquad \Delta = \ln\beta(l_1) - \ln\beta(0) \tag{6}$$

$$\approx \mathcal{V}_{\parallel}\,\tau\,\xi^2 \tag{7}$$

Speedup by field line reconstruction

- Magnetic field lines are reconstructed from a field aligned grid, which allows a significant speedup of the parallel motion of particles.

- Bilinear interpolation between 4 pre-defined field lines $\mathbf{F}_i(\varphi)$ at the position (ξ, η, φ) of a simulation particle:

$$\mathbf{F}^*_{\xi,\eta}(\varphi) = \sum_{i=1}^{4} \mathbf{F}_i(\varphi)\, N_i(\xi, \eta)$$

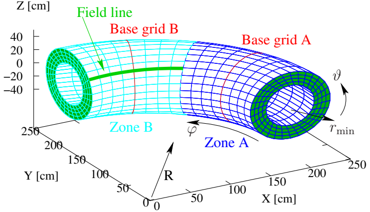

where

$$N_i = \frac{1}{4}(1 + \xi_i\, \xi)(1 + \eta_i \eta)$$

are shape functions (known from Finite Element Methods) and ξ, η are field line labels.

- Grid cells must be convex for a unique relation $(R, Z) \leftrightarrow (\xi, \eta)$, therefore toroidal sub-domains are necessary.

Even the 2PM exhibits bifurcations and oscillations

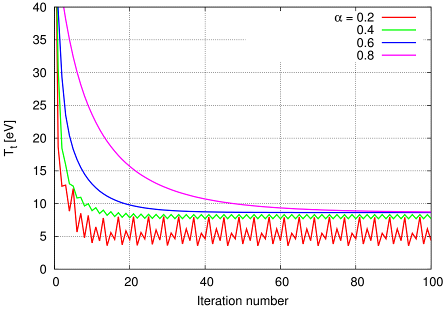

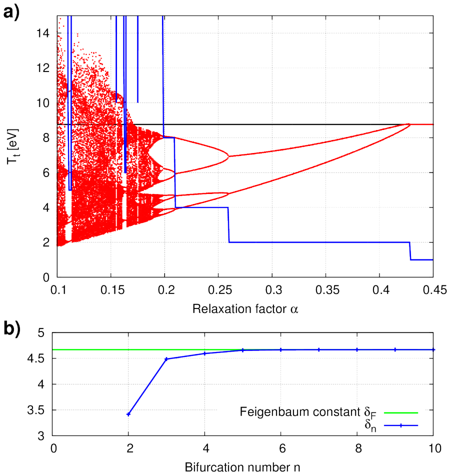

2PM analysis

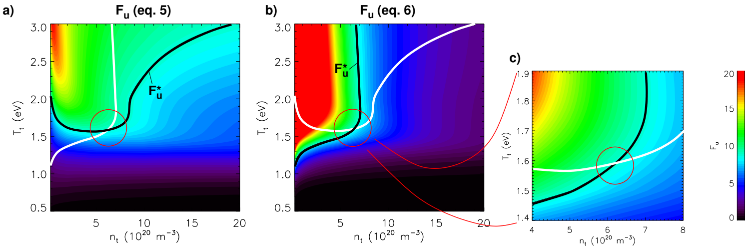

$$T_u \approx \underbrace{\left(\frac{7\, q_\parallel\, L}{2\, \kappa_{0e}}\right)^{2/7}}_{=T_{u0}} f_{\text{cond}}^{2/7}$$

$$T_t = \underbrace{\frac{m}{2\, e}\, \frac{4\, q_\parallel^2}{\gamma^2\, e^2\, n_u^2\, T_{u0}^2}}_{=F_u}\, \frac{(1 - f_{\text{power}})^2}{f_{\text{mom}}^2\, f_{\text{cond}}^{4/7}}$$

$$n_t = \frac{f_{\text{mom}}\, n_u\, T_u}{2\, T_t} = \frac{n_u\, T_{u0}}{2\, F_u}\, \frac{f_{\text{mom}}^3\, f_{\text{cond}}^{6/7}}{(1 - f_{\text{power}})^2}$$

$$f_{\text{power}} = \varepsilon(n_t,\, T_t)\, \Gamma_t\, q_\parallel$$

$$f_{\text{mom}} = 1 - \exp(-\Delta X_\perp / \lambda), \qquad \lambda = \frac{v_{th}}{n_t\, \langle \sigma_{\text{iz}}\, v \rangle}$$

$$f_{\text{cond}} = 1 - \left(\frac{T_t - T_c}{T_c}\right)^2 \text{ for } T_t < T_c = 4\,\text{eV}$$